

Effect of Iron Phase Evolution on Copper Separation from Slag *Via* Coal-Based Reduction



SHIWEI ZHOU, YONGGANG WEI, BO LI, and HUA WANG

Copper slag, a by-product of copper pyrometallurgy, inevitably contains a certain amount of copper. Oxygen-enriched smelting technologies increase the copper content in slag indirectly because of the production of higher-grade matte. The effect of iron phase evolution on the copper content in slag during the slag cleaning process in an electric furnace was investigated using the method of combining theory with experiments. Based on the analysis, the main factors that impede the separation of slag and copper/matte were determined. Subsequently, the properties of slag were analyzed after decreasing the magnetite content within the slag. The experimental results showed that decreases in magnetite content were beneficial for the separation of copper and slag because of the decrease of slag viscosity. Nevertheless, Cu-Fe alloys formed when magnetite was completely reduced to metallic iron, and the foaming slag was formed at 1250 °C. Furthermore, the distribution of copper in the reduced slags was studied in detail.

<https://doi.org/10.1007/s11663-018-1379-4>

© The Minerals, Metals & Materials Society and ASM International 2018

I. INTRODUCTION

THE special physicochemical properties of copper determine its extensive applications; currently, copper is mainly used in the building and power industries. Because of the shortage of copper ore, the development of copper resources is gradually transferring to secondary resources, such as end-life printed circuit boards and slag.^[1,2] Nevertheless, copper is primarily produced by pyrometallurgy methods^[3] such as Isa smelting, Outokumpu flash smelting, Inco flash smelting, Noranda reactor, Teniente reactor, Mitsubishi continuous smelting and other bath smelting. As a raw material, copper sulfide concentrates typically contain 25 to 30 pct Cu, 28 to 34 pct Fe and 28 to 34 pct S.^[4] In the process of matte making, the intense chemical reactions in the bath occur at approximately 1523 K (1250 °C), and part of the iron sulfide oxidizes and reacts with silica to form fayalite slag. The matte obtained from such smelting is then transferred into the converter for converting blister copper.

Oxygen-enriched bath smelting technology has the advantages of high efficiency, environmental protection and automation, and it is widely applied to matte and/or blister copper smelting. However, the oxygen potential increases in the bath by oxygen-enriched blowing, which leads to the increase of magnetite content in slag; the copper content in slag increases as a result. Approximately 68.7 million tons of copper slag are produced annually worldwide by copper smelting plants,^[5] and the copper losses in these slags cause significant ecologic and economic issues and are encountered in all copper smelting techniques. Generally, the copper content in slag is approximately 0.7 to 2.3 wt pct.^[6] Copper is lost to slag by the following two processes: (1) physicochemical losses are related to dissolved copper species (Cu₂O, Cu₂S) in slag;^[4,7,8] (2) mechanical entrained losses, primarily due to high slag viscosity, are the main form of copper loss for the lower matte grades (wt pct Cu < 60).^[6] Based on previous studies, the main factors affecting the copper content within slag can be attributed to the following aspects: matte grade, temperature, oxygen potential, slag composition and other properties.^[9-12] High efficiency slag-matte separation can be achieved by controlling the slag composition in the smelting stage. The surface tension of slag increases with the additions of CaO, MgO and Al₂O₃, and the viscosity decreases with the addition of CaO^[7]; both of these results are beneficial for separation. In addition, Rusen *et al.*^[6] investigated the effect of CaO, colemanite and B₂O₃ on copper losses to smelting slag and concluded that copper losses increased by increasing the addition of CaO and B₂O₃ above 4 wt pct.

SHIWEI ZHOU, BO LI, and HUA WANG are with the Faculty of Metallurgical and Energy Engineering, Kunming University of Science and Technology, Kunming 650093, P.R. China. YONGGANG WEI is with the State Key Laboratory of Complex Nonferrous Metal Resources Clean Utilization, Kunming University of Science and Technology, Kunming 650093, P.R. China. Contact e-mails: weiygcp@aliyun.com, wanghua65@163.com

Manuscript submitted March 20, 2018.

Article published online August 9, 2018.

The matte obtained from the smelting operation is processed in converters for the production of blister copper, in which the iron sulfide in the matte is oxidized by oxygen-enriched air. Thermodynamic modeling [specific parameters: Fe/SiO₂, matte grade, partial pressure of SO₂, and minor oxide levels in slag (CaO, MgO, Al₂O₃ and ZnO)] was performed by Cardona *et al.*^[15] to evaluate the chemistry and copper losses in converter slag. However, all of the above parameters may not occur simultaneously in a smelting furnace. In general, the converter copper slag contains a high copper content (commonly 2 to 8 wt pct Cu^[4]; partial slag containing copper is up to 20 pct) due to the higher matte grade and slag viscosity. This part of slag, therefore, needs to be recycled for the further treatment of recovery copper. Magnetite is considered to be the main factor affecting the copper content in the slag because of its higher melting point and stable chemical properties. The pyrometallurgy method of reducing slag in an electric furnace is widely used to promote the separation of slag and matte/copper.^[14–17] The smelting parameters (temperature, electrode power density, coke addition and so on) have been investigated to promote the reduction rate of slag^[17]; the external magnetic field can cause slag stirring, which could promote the aggregation of copper and slag reduction.^[18–20]

From the viewpoint of slag reduction, very few studies have attempted to investigate the effect of iron phase transformation on the copper content in slag. The reduction kinetics of fayalite slag were investigated for determining the restrictive control steps, and the results show that the fayalite slag reduction is first controlled by the Boudouard reaction and then by mass transfer.^[21–23] Additionally, the studies that have been carried out predominately concentrated on the recovery of iron from copper slag.^[24–27] Therefore, in the present study, the effect of chemical reactions of the iron phase on copper separation from converter slag was investigated during the slag cleaning process in electric furnaces; the corresponding microstructures of the slag layers were studied in detail. Furthermore, the behavior of the settlement and aggregation of copper particles in slag was determined. The results obtained may provide a theoretical basis for the prevention of excessive reduction of iron in the process of industrial slag cleaning in electric furnaces.

II. EXPERIMENTAL

A. Materials

PS converter slag was used as an experimental subject to investigate the effect of iron phase transformation on copper separation from slag during the slag cleaning in an electric furnace. A representative converter slag sample was supplied by Yunnan Copper Inc. After grinding and mixing of the slag, a chemical analysis was used to determine the composition, and the results are shown in Table I. Converter copper slag had 4.49 wt pct

Cu, 44.91 wt pct Fe, 0.53 wt pct S and 21.04 wt pct SiO₂. According to the analysis, copper exists mainly in the form of metallic Cu within slag. In addition, the magnetite content in the slag was detected by a magnetic analyzer, and the value was 34.1 wt pct. Anthracite was used as a reductant, and its chemical composition is given in Table II. The slag and anthracite were ground using an XZM-100 laboratory vibratory mill until 98 pct of the particles were < 74 μm prior to conducting the experiments.

Figure 1 shows the X-ray power diffraction (XRD) pattern, which identifies fayalite and magnetite as the main phases of the copper slag. As noted in Table I, oxides such as CaO, MgO and Al₂O₃ were identified in the chemical analysis of the slag; however, these oxides were not observed in the XRD pattern. These results are consistent with results reported elsewhere.^[6]

B. Apparatus and Procedure

A series of reduction experiments was carried out in a vertical tube furnace using corundum crucibles; the schematic of the experimental furnace is shown in Figure 2. First, a prepared copper slag sample with a certain amount of reductant was homogeneously mixed in a laboratory rotary mixing drum and placed in a corundum crucible (30 ± 1 mm inside diameter). The crucible was then placed in the constant-temperature zone of the tube furnace. The corundum reaction chamber of the furnace was evacuated using a mechanical rotary pump; nitrogen gas was then introduced (100 ml/min) and controlled by a rotameter. The furnace was heated to 1523 K (1250 °C) at a constant heating rate of 10 K min⁻¹ while maintaining the nitrogen atmosphere. The sample was held at the required time in the nitrogen atmosphere and then quickly cooled. After separation from the crucible, the slag was analyzed by several different techniques including a wet chemical analysis, saturated magnetite analysis, X-ray power diffraction and electro-probe microanalysis (EPMA).

The samples were initially ground, and the magnetite content was obtained by a magnetic susceptibility measurement using a Satmagan S135 instrument with an accuracy of 0.4 wt pct of the measured values. For mineralogic characterization of the slag sample, a Japan Science D/max-R diffractometer (Rigaku MiniFlex 600) was used to confirm the identity of the solid phase. The diffractograms were measured in the 20 to 80 deg 2θ range and used a step size of 0.01 deg (Cu Kα radiation generated at 40 kV and 40 mA). To obtain information about the microstructure and component distribution of the slag sample, the EPMA was carried out using a JEOL JXA 8230 model equipped with energy-dispersive X-ray spectroscopy. In addition, thermochemical analyses of the FeO-Fe₃O₄-SiO₂ and Cu-Fe system at different temperatures were calculated and plotted as ternary and binary phase diagrams by using the phase diagram module of the FactSage^{6,2} thermochemical software.

Table 1. Chemical Analysis of the Slag Sample

Component	Cu	S	Fe (Total)	Zn	Al ₂ O ₃	SiO ₂	CaO	MgO	Fe ₃ O ₄
Content Weight Percent	4.49	0.53	44.91	3.88	2.57	21.04	0.86	0.61	34.1

Table II. Industrial Analysis of the Reductant

Properties	Fixed Carbon	Volatile Matter	Ash	Moisture
Content (Weight Percent)	76.43	7.78	15.29	1.02

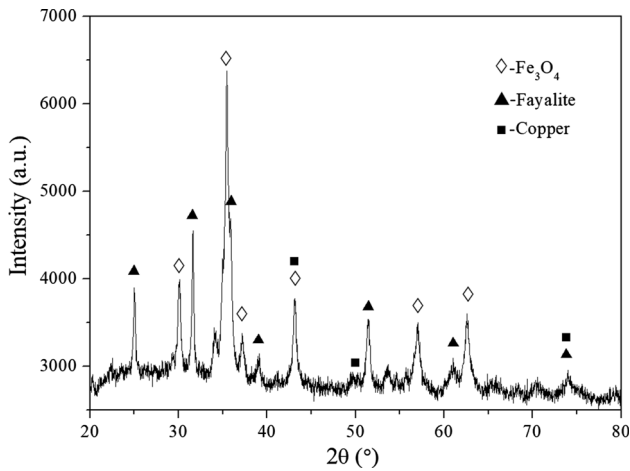


Fig. 1— XRD pattern of the copper slag sample.

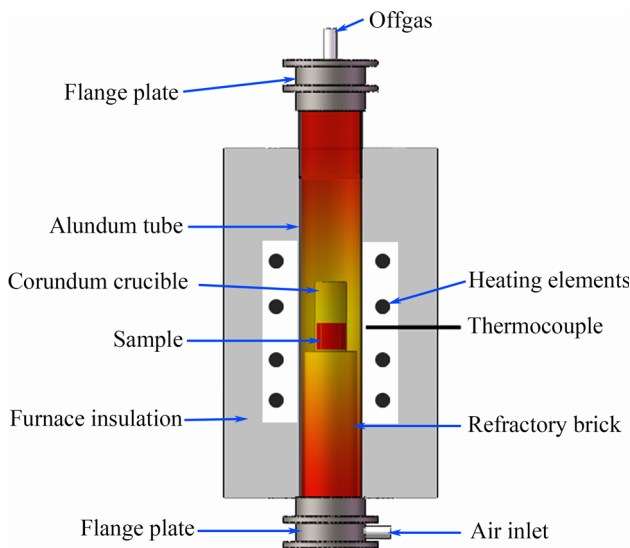
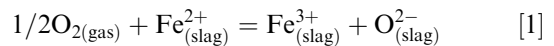


Fig. 2— Schematic of experimental furnace.

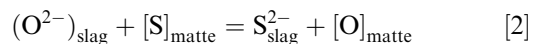
III. RESULTS AND DISCUSSION

A. Analysis of the Copper Matte Converting Process

The copper matte converting process can be divided into two stages: the slag making stage and blister converting stage. The iron phase, which primarily exists in copper matte as iron sulfide (FeS), is first oxidized to FeO and then combined with SiO₂ to form fayalite. When FeS is thoroughly oxidized, the matte converting process is transferred from the slag making stage to blister converting stage, and Cu₂S begins to oxidize to produce metallic copper. In the process of copper matte converting, the system in the furnace is usually a triphase coexistence (gas-slag-matte).^[28] The oxygen potential in the gas and slag phase is higher than that in the matte, while the sulfur potential is lower than that in the matte phase. Thus, the high oxygen potential in the gas (or slag) inevitably transfers oxygen to the matte, and the sulfur potential in the molten matte inevitably transfers sulfur to the slag and/or gas. Therefore, the process of copper matte smelting is essentially a substitution process of sulfur and oxygen, and the difference of sulfur and oxygen potentials in the coexisting system promotes the development of this substitution process. The exchange model of oxygen and sulfur in the copper matte converting process is illustrated in Figure 3. In the initial stage of blowing smelting, oxygen in the gas first diffuses into the slag and oxidizes Fe²⁺ to Fe³⁺ in the slag, which simultaneously produces O²⁻:



The process described in the reaction above results in the increase of oxygen in the slag, further increasing the oxygen concentration and leading to the transfer of oxygen ions from the slag to the matte layer:



With the transfer of oxygen ions from the slag to the matte layer, anions from the matte layer must be transferred to the slag layer. Because the oxygen ions that entered the matte layer are attracted to the Fe²⁺/Cu²⁺, free sulfur ions are transferred to the slag because of the positive charge and low sulfur potential in the slag layer. Sulfur in the slag layer diffuses to the gas and is oxidized to form sulfur dioxide as follows:

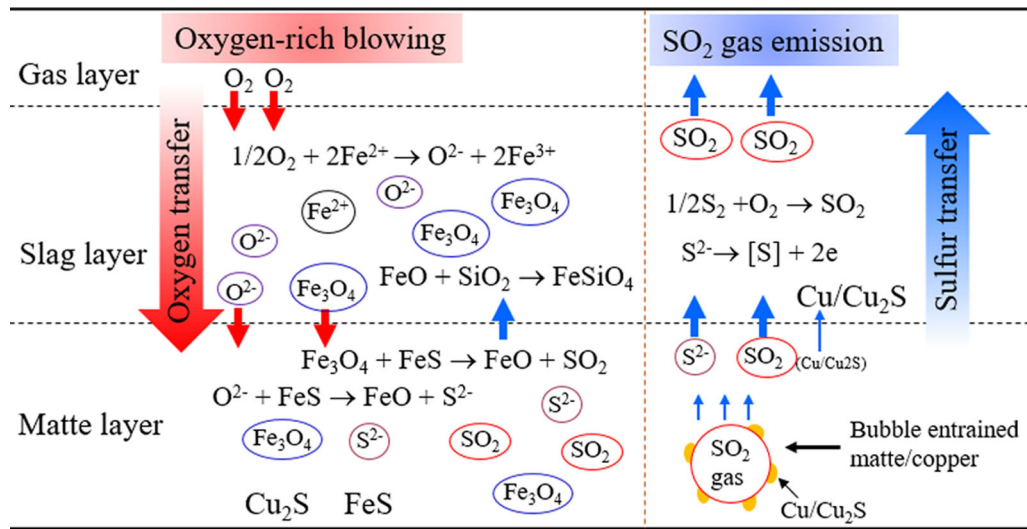
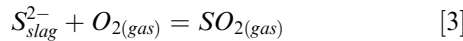


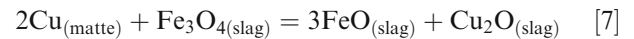
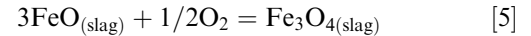
Fig. 3— The exchange model of oxygen and sulfur in the copper matte converting process.



For the system equilibrium, the diffusion of oxygen increases the oxygen concentration in matte. Iron, which is more electronegative than copper, is preferentially oxidized into the slag phase, which is shown in Reaction [4].



As the oxygen potential increases, the rate and quantity of oxygen and sulfur ion transfer also increase; as a result, the converting process is strengthened. However, as the oxygen potential increases, the FeO in slag oxidizes to magnetite [Reaction 5]. As the reaction proceeds, the activity of FeO decreases, whereas the activity of magnetite increases. When the content of silica or the temperature is low, the magnetite readily precipitates from the slag [Reaction 5]. In contrast, in the case of higher silica content, silica precipitates from the slag.^[29] In the molten slag, silica exists in the form of a complex silicon/oxygen anion with a SO_4^{4-} constitutional unit; its structure is complex and its ionic radius is large.^[30] Such a large complex anion migrates from one position to another in the flow; that migration requires a significant energy input resulting in high viscosity. Further increases in the oxygen potential result in the precipitation of solid state magnetite. Solid magnetite is suspended in the matte because of its density and reacts with cuprous sulfide (Cu_2S) to generate SO_2 gas [Reaction 6]. When the SO_2 gas diffuses from the matte, it takes away a portion of the matte/copper particles into the slag layer, resulting in copper mechanical losses. Accordingly, the precipitation of magnetite and/or silica is detrimental to the copper smelting process. Furthermore, part of the metallic Cu generated [Reaction 6] dissolves in the matte; another part oxidizes to form Cu_2O and results in a chemical loss to slag [Reaction 7].



B. Cu Separation from Slag During the Slag Cleaning Process

At high temperatures, the appetency between iron and oxygen surpasses that of copper and oxygen. The formation of Fe_3O_4 is therefore inevitable during the converter blowing process of copper matte. Table I shows that the Fe_3O_4 content in converter slag is approximately 34.1 wt pct. The influence of magnetite on slag can be summarized as follows: (1) Fe_3O_4 in slag exists primarily in the form of solid particles because of its high melting point, which leads to an increase in slag viscosity. Furthermore, the increase of slag viscosity increases the mechanical entrainment loss of copper; (2) the presence of magnetite in the slag indicates that the oxygen potential is high, which results in the increase of chemical losses of copper. Therefore, the reduction of magnetite in the process of copper slag cleaning in an electric furnace for increasing copper recovery is inevitable.

1. Reducing Fe_3O_4 to FeO

The proper amount of reducing agent can reduce magnetite to ferrous oxide. The viscosity of slag is related to the composition and temperature of slag. Based on *FactSage* software calculations, decreases in viscosity are observed at all temperatures as the amount of FeO increases (Figure 4). The copper slag used in this study was a silica-saturated slag. As indicated previously, silica exists in the form of a complex silicon

oxygen anion with a SO_4^{4-} constitutional unit; Bockris *et al.* proposed the depolymerization concept of the complex three-dimensional silicate network to account for the viscous flow behavior of CaO-SiO_2 based melts.^[31] As Fe^{2+} is gradually introduced, the complex silicate network structure decomposes into a simpler structure, which results in decrease in slag viscosity. When a sufficient amount of Fe^{2+} is introduced, the silicate anions approach their lower size limit, and the viscosity tends to reach a plateau, as shown in Figure 4. Moreover, the slight temperature dependency of the viscosity found at high concentrations of Fe^{2+} may be

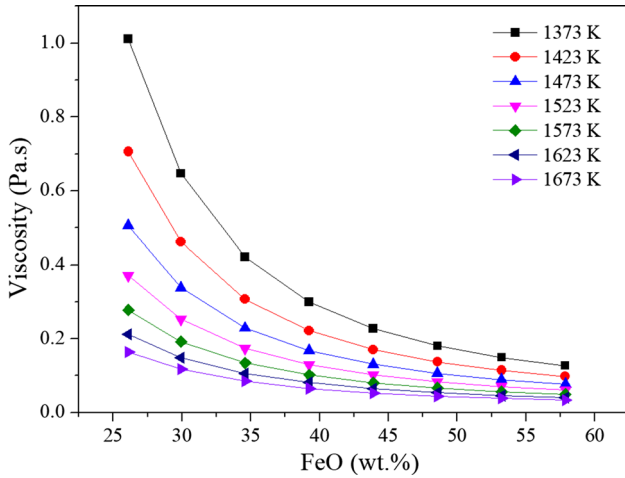


Fig. 4— Effect of FeO content on the viscosity of slag.

due to the lower size limit, such that an increase in temperature would not result in further depolymerization.^[32]

The phase diagram of the $\text{FeO-Fe}_3\text{O}_4\text{-SiO}_2$ system is calculated by *FactSage* software and is shown in Figure 5, which indicates that a smaller liquid phase exists around the crystalline region of fayalite and reduces the solubility of Fe_3O_4 . According to the slag composition, the composition position is located in the spinel phase region at 1523 K (1250 °C) (Figure 5), leading to a higher viscosity of molten slag. Nevertheless, as the amount of Fe_3O_4 decreases, the slag component position gradually approaches the liquid phase region. In addition, the liquid region increases gradually as the temperature increases, as shown in Figure 5(b).

The results of the copper content in slag reduced at 1523 K (1250 °C) for 1 min as a function of coal dosages (ranging from 0 to 2.4 wt pct) are depicted in Figure 6. The magnetite content obviously decreased as the reductant dosage increased; those results are shown in Figure 6. Based on the theoretical calculation, approximately 2.3 wt pct of coal is needed to completely reduce the magnetite to form FeO within slag. When the reductant dosage increases from 0 to 2.3 wt pct, the Fe_3O_4 and Cu contents significantly decrease from 34.1 and 4.49 wt pct to 0.6 and 1.00 wt pct, respectively. With the decrease of magnetite content in slag, the $\log p\text{O}_2$ value is calculated by Eq. [8],^[33] and the results are shown in Figure 6(b). The $\log p\text{O}_2$ of a smelting system is essentially fixed by the compositions of the oxidizing medium.^[34] For a fixed pct Fe/ pct SiO_2 and temperature, a higher concentration of $[\text{Fe}^{3+}/\text{Fe}^{2+}]$ increases the $\log p\text{O}_2$. Thus, Figure 6(b) shows the decrease in the $\log p\text{O}_2$ as the magnetite content decreases.

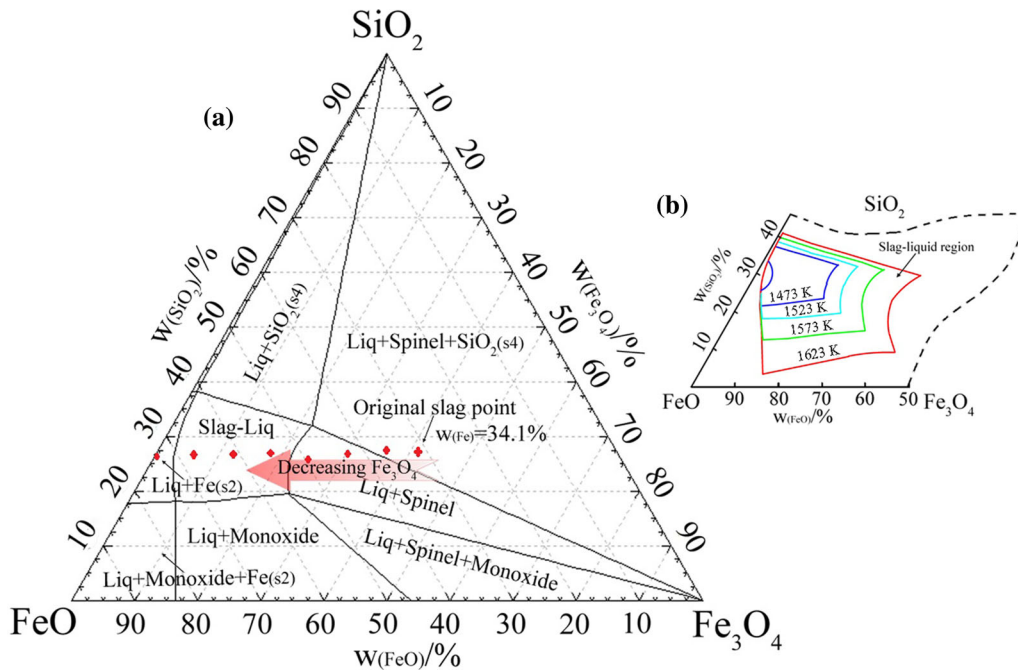


Fig. 5— Phase diagram of the $\text{FeO-Fe}_3\text{O}_4\text{-SiO}_2$ ternary system (a); the slag-liquid region at various temperatures (b).

$$\log p_{O_2} = 16.3 + 4 \log [Fe^{3+}/Fe^{2+}] - \text{pct Fe}/\text{pct SiO}_2 - 29500/T \quad [8]$$

where $[Fe^{3+}/Fe^{2+}]$ represents the ratio of ferric and ferrous iron concentrations, and $\text{pct Fe}/\text{pct SiO}_2$ is the mass ratio of the iron and SiO_2 .

Meanwhile, the corresponding XRD patterns (Figure 7) show that the intensity of the magnetite diffraction peaks gradually weaken as the reductant dosage increases from 0.4 to 2.4 wt pct, in line with the results depicted in Figure 6; conversely, the intensity of the wustite diffraction peaks varies in an opposite trend. Specifically, as the reductant dosage increases, the fayalite diffraction peaks become more intense but then gradually decrease. The magnetite can be reduced to form wustite under weak reducing conditions, which react with SiO_2 to generate fayalite. As the conditions become more reducing, some fayalite is reduced to wustite, resulting in the decrease in fayalite peaks. In

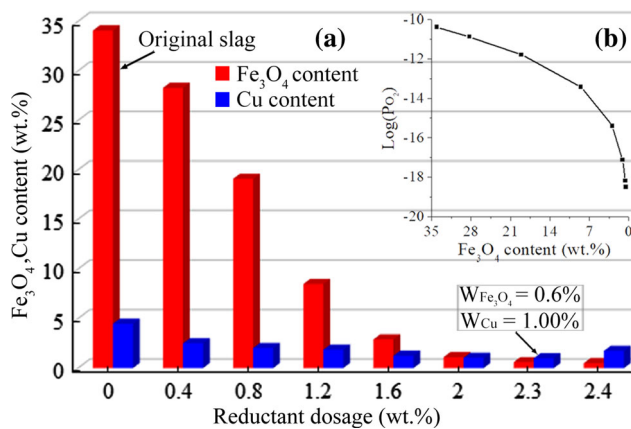


Fig. 6— Effect of the reductant dosage on Fe_3O_4 and Cu contents in slag (a); $\log(p_{O_2})$ values with various Fe_3O_4 contents (b).

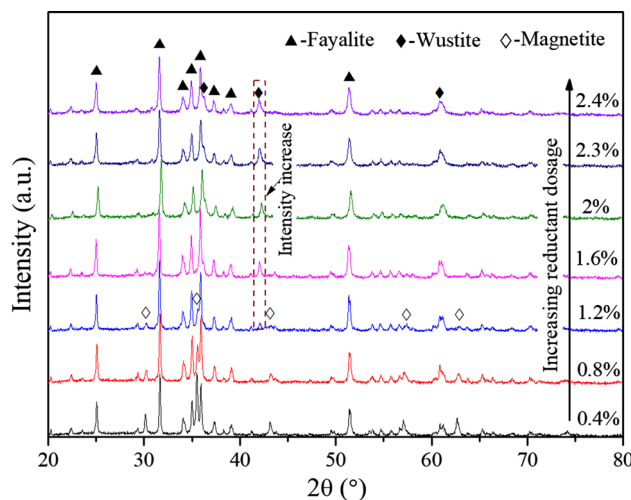


Fig. 7— XRD patterns of the slag sample after reduction with various reductant dosages.

addition, the reasons for the decrease of the copper content in slag may be summarized as follows: (1) as mentioned above, a decrease in the amount of Fe_3O_4 could also decrease the slag viscosity, which promotes the separation of copper from slag; (2) the oxygen potential of the slag decreases with the decrease in magnetite content in slag, which results in the decrease of the chemical dissolution of copper in slag; (3) the copper surface tension increases with a decrease in the oxygen potential,^[35] which is advantageous for the separation of slag and copper. Nevertheless, as the conditions become more reducing, magnetite content in slag continues to decrease, such that the Cu content increases from 1.00 to 1.74 wt pct.

The effect of the reduction time on Cu content in slag was investigated to further separate the copper from slag, and the results are shown in Figure 8. Figure 8 shows that the Cu grade in slag reaches a minimum value of 0.32 wt pct when the reduction time increases from 1 to 10 minutes. The Cu content then increases as the reduction time increase beyond 10 minutes. Prolonging the reduction time is beneficial for Cu separation from slag; however, the solubility of copper in slag also increases as the reduction time is extended. Figure 9 shows the slag sample after reduction at various times. The metallic copper particles are distributed in the upper part of the slag and bottom of the crucible, as shown in Figure 9(a). The vast majority of copper settles and forms copper ingots during the reduction process (Figure 9). Three copper particles are visible at the bottom of the crucible when the settlement time is 1 minute (Figure 9(a)). Extending the settlement time results in gradual aggregation of the smaller copper particles into larger particles (Figure 9(b, c)), indicating that the copper particles settled prior to the aggregation during the reduction process. Nevertheless, a small amount of copper particles is still observed in the upper part of the slag layer in Figure 9(a). In the reduction process, the generation of gas bubbles resulted from chemical reactions between iron oxide and the carbon (Eq. [9]). The bubbles generated at the interface between the Cu droplets and slag may provide sufficient upward

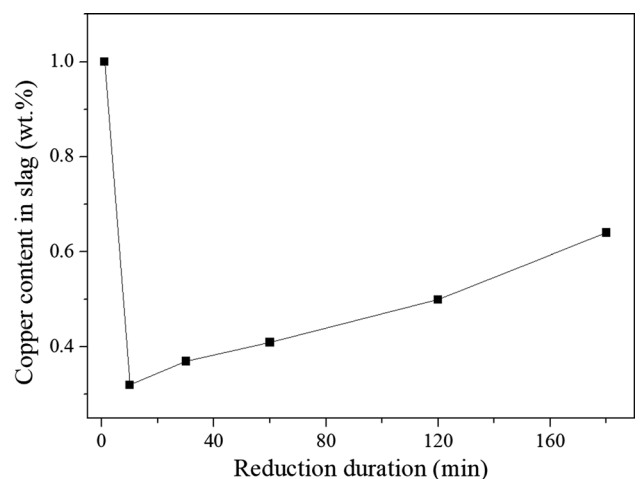
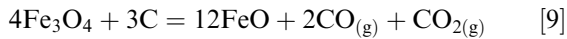


Fig. 8— Effect of reduction duration on Cu content in slag.

force (buoyancy) to cause the metallic copper droplets to float up instead of settle to the bottom,^[36] resulting in visible copper particles on the slag surface. This is also one of the reasons for mechanically entrained copper in slag.



2. Reducing FeO to Fe

Excess reductant reduces ferrous oxide and fayalite to metallic iron. As mentioned above, approximately 2.3 wt pct anthracite is needed to completely reduce the magnetite to ferrous oxide. Further increasing the amount of reductant also increases the copper content in slag, as shown in Figure 6. The slag sample in the crucible after the smelting reduction with 4 wt pct of added anthracite is shown in Figure 10; it clearly shows that the copper droplets do not settle to the bottom of the crucible to form metallic copper ingots such as the slag sample shown in Figure 9. In addition, the slag sample shows obvious stratification in the crucible. The upper layer has loose structure characteristics, and the corresponding XRD pattern is shown in Figure 10(b). The primary phase, which is evident from the XRD

pattern of the slag sample, is fayalite, and the minor phases are iron and copper. For the lower layer, the structure is compact, and the XRD result shows that fayalite is the main phase, indicating that the lower part may be the slag phase with fayalite as the matrix. The main reason for the structural differences between the upper and lower layers may be attributed to the generation of reducing gas. While the reducing gas escapes, ferrous oxide in contact with CO is reduced to metallic iron, which is combined with copper to produce an alloy. In the current experimental conditions, Fe-Cu alloy is difficult to melt, resulting in a foaming upper slag layer.

The EPMA method was used to further investigate the corresponding microstructure and composition of the two slag layers. Figure 11 presents the EPMA images of the upper reduced slag sample (loose structure part) at 1523 K (1250 °C) for 1 minute with the addition of 4 wt pct anthracite. Figure 11(b) provides a magnified view of the marked areas in Figure 11(a). As seen from the SEM image (Figure 11a) coupled with the WDS results, the charcoal gray and white gray substances are the fayalite and Cu-Fe alloy, respectively. The alloy is formed by the combination of copper and metallic iron

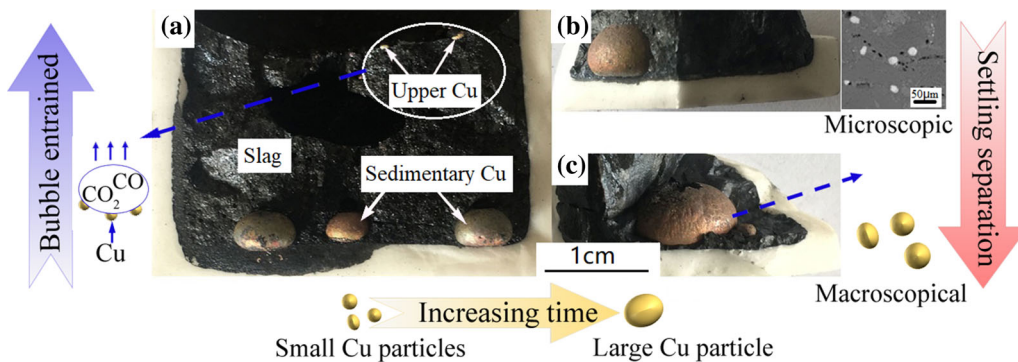


Fig. 9— Images of the slag sample after reduction at 1523 K (1250 °C) with a 2.3 wt pct reductant dosage for various durations: (a) 1 min; (b) 10 min; (c) 180 min.

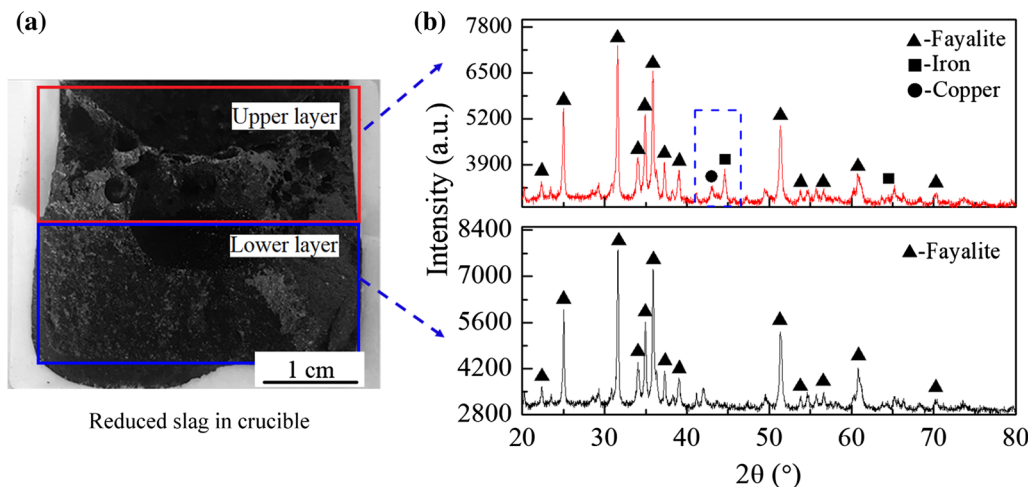


Fig. 10— Image of the slag sample (a) and its XRD pattern reduction at 1523 K (1250 °C) with a 4 wt pct reductant dosage (b).

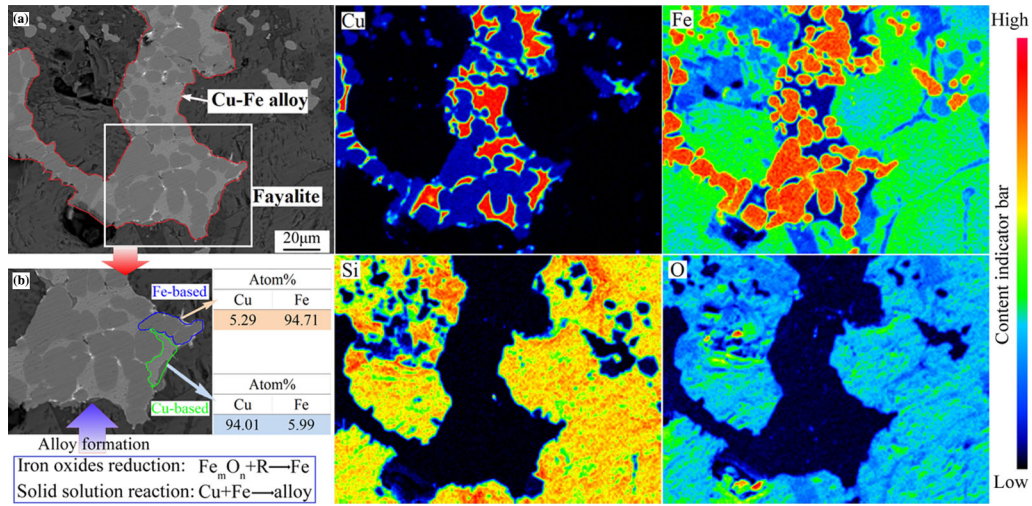


Fig. 11— EPMA images of the upper slag layer (a), reduced at 1523 K (1250 °C) for 1 min with a 4 wt pct reductant dosage; (b) magnified view of the marked areas in (a).

produced by the reduction process at high temperature. The Cu-Fe alloy has large particle sizes and is connected to the fayalite. In particular, Figure 11(b) shows the details of the Cu-Fe alloy particles, demonstrating that the two phases exist in the Cu-Fe alloy. Based on the component analysis, the matter with lighter color is the Cu-based alloy, whereas the round particles with darker color correspond to the Fe-based alloy. As seen from the binary phase diagram of Cu and Fe (Figure 12), Cu and Fe both have the characteristic of miscible dissolution due to their similar chemical structure. However, the Cu-Fe alloy cannot be completely melted into liquid phase, resulting in its uneven chemical composition. At 1523 K (1250 °C), when the copper content is higher than 92.33 wt pct, the alloying components are primarily in the liquid phase; this theoretical analysis explains the morphology of the Cu-based alloy, which has no fixed shape (Figure 11(b)). However, as the Fe content increases to 91.56 wt pct, the components exist in the presence of the γ -Fe phase. Thus, the two components have different morphologies in the SEM images.

Figure 13 shows the SEM-EDS results of the lower reduced slag sample (compact structure part). Figure 13(b) is the magnified view of the marked areas in Figure 13(a). As seen in Figure 13(b) and coupled with the EDS results, the following three phases are clearly observed: the charcoal gray, white gray and light gray phases are the fayalite, Cu-Fe alloy and iron oxide, respectively. Fayalite is the primary phase in the lower part of the slag sample, which agrees with the XRD results. The details of the Cu-Fe alloy particles are similar to the results described in the previous section. Nevertheless, in contrast to Figure 11, Figure 13(a) shows that the alloy is present in lower concentrations and smaller particle sizes. In addition, the iron oxide phase found in the lower part may be attributed to the reductant dosage. Based on the theoretical calculation, approximately 9.3 wt pct anthracite is needed to completely reduce the magnetite to metallic iron. At present, the reductant dosage is 4 wt pct; therefore, a portion of magnetite is not reduced to metallic iron

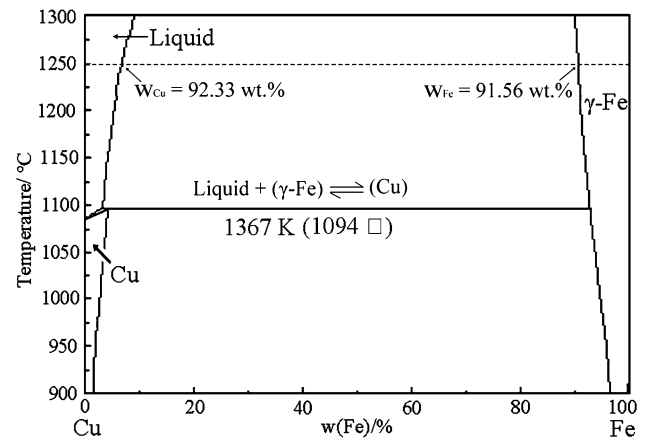


Fig. 12— Phase diagram of the Cu-Fe binary system.

As the reductant dosage increases, the loose structure of the upper slag layer gradually increases, indicating the formation of foaming slag during reduction; the corresponding lower fayalite layer (compact structure) decreases as a result, as shown in Figure 14. The reason for this result may be ascribed to the reductant gas as described previously. From the thermodynamic viewpoint, the iron oxide and fayalite are reduced to form metallic iron by excessive reductant (anthracite and CO gas), destroying the equilibrium of the slag phase. Furthermore, the high melting point of metallic iron causes the caking of slag. To further investigate the effect of the reduction time on copper within the slag, an experiment was performed with the following reduction conditions: reduction duration of 60 minutes, 6 wt pct reductant dosage and temperature of 1523 K (1250 °C). The stratification of slag is also observed, and the two layers were analyzed by SEM as shown in Figure 15. In contrast to Figure 11, there is no obvious difference in the microstructure and composition of the upper slag in addition to the well-crystallized fayalite phase (Figure 15(a)). Nevertheless, as seen from the lower layer SEM image (Figure 15(b)) coupled with the EDS

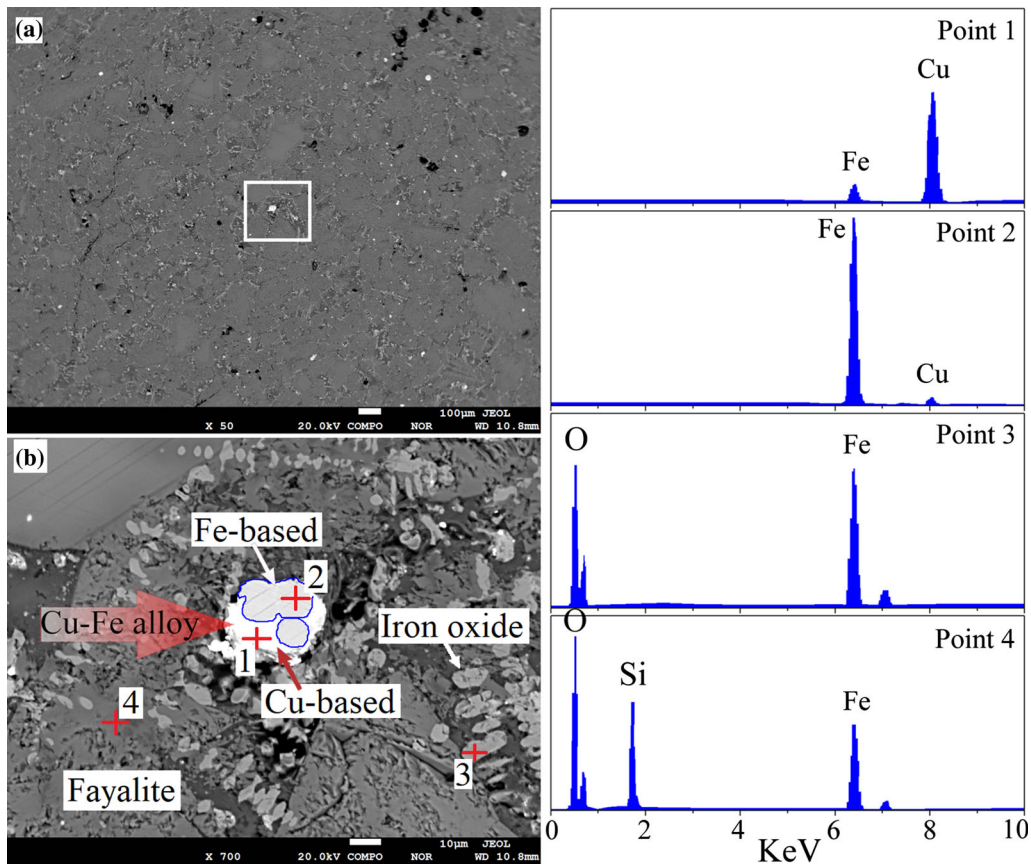


Fig. 13— EPMA images of the lower slag layer (a) reduced at 1523 K (1250 °C) for 1 min with a 4 pct reductant dosage; (b) magnified view of the marked areas in (a).

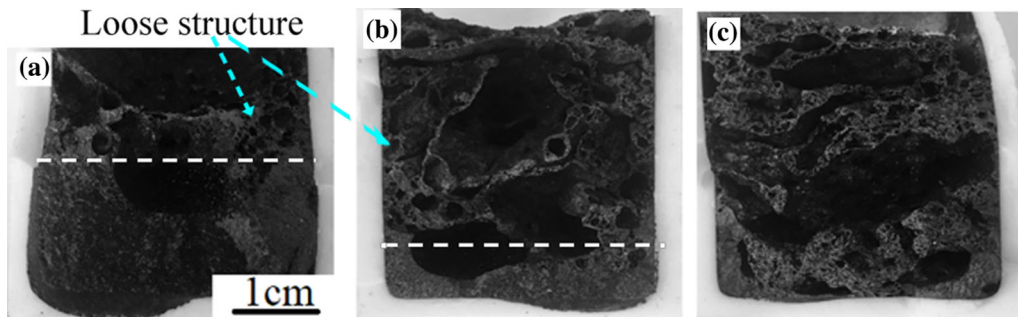


Fig. 14— Images of the slag sample after reduction at 1523 K (1250 °C) with various reductant dosages for 1 min: (a) 4 wt pct reductant dosage; (b) 6 wt pct reductant dosage; (c) 8 wt pct reductant dosage.

results, the precipitated matte particles are observed and appear as sulfide dots of $< 10 \mu\text{m}$ dispersed in the glassy matrix. This finding, consistent with other research results,^[37] may be attributed to the exsolution of the dissolved matte with the decrease in oxygen potential and temperature. Furthermore, minor elements (As, Sb, Bi and Pb) are always present in sulfide concentrates,^[38,39] such as matte. Figure 15(b) shows a matte particle containing lead. Combined with the above analysis, the copper reacts with metallic iron to form an alloy and is distributed in the upper layer of slag, which readily causes the formation of foaming slag in

the furnace. Furthermore, in the actual process of copper smelting, the dissolution of iron in copper solution is not advantageous for the refining of blister copper.

IV. CONCLUSIONS

In the present study, the smelting reduction method was used for slag cleaning. In the process of reducing magnetite to ferrous oxide, the copper particles primarily aggregated and settled to the bottom of the crucible

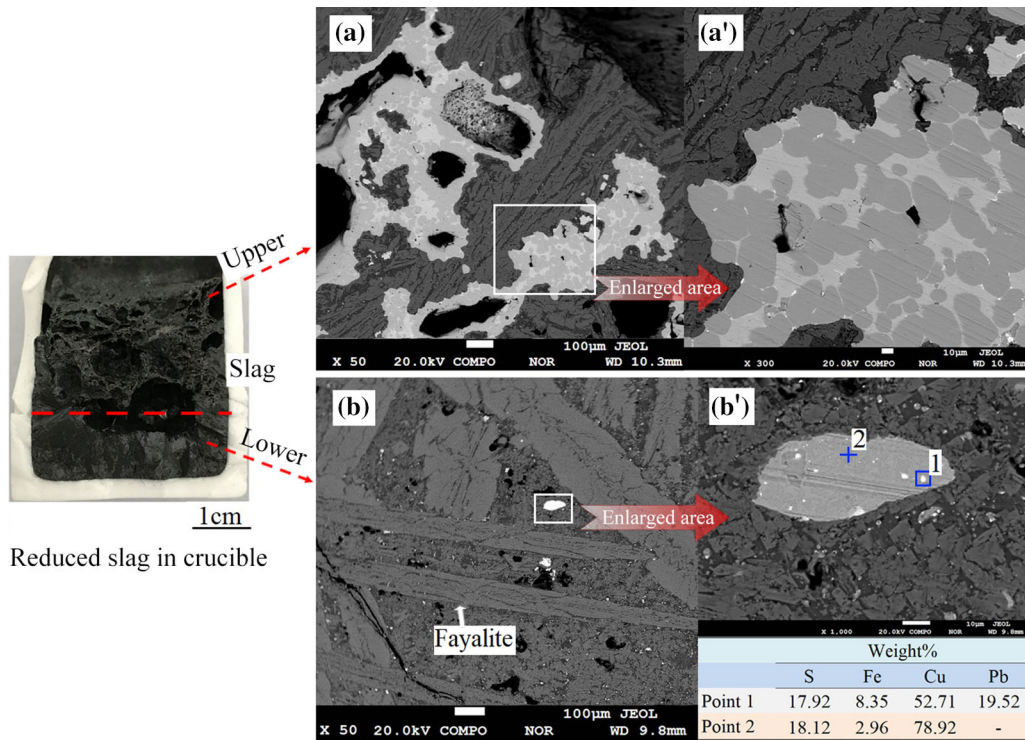


Fig. 15— Image of the slag sample after reduction at 1523 K (1250 °C) with a 6 wt pct reductant dosage for 60 min: (a) microstructure of the upper slag layer; (b) microstructure of the lower slag layer.

to form a copper ingot. The copper content in slag was reduced from 4.49 to 0.32 wt pct *via* the smelting reduction at 1523 K (1250 °C) for 10 minutes in the presence of 2.3 wt pct anthracite. When the magnetite was reduced to metallic iron, the copper slag had a distinct stratification; the upper layer slag formed foaming slag, and the lower layer was dense. Metallic copper formed alloys with iron and was mainly distributed in the upper slag. These results imply that the generation of metallic iron would lead to the formation of foaming slag, which is not conducive to the separation of slag and copper during the slag cleaning process. The excessive reduction of magnetite in the slag should be avoided in the actual production process for slag cleaning in electric furnaces.

ACKNOWLEDGMENTS

This work was supported by the National Natural Science Foundation of China (U1602272 and 51664039) and the Analysis and Testing Foundation of Kunming University of Science and Technology (2017P20161102004).

REFERENCES

1. I.F.F. Neto, C.A. Sousa, M.S.C.A. Brito, A.M. Futuro, and H.M.V.M. Soares: *Sep. Purif. Technol.*, 2016, vol. 164, pp. 1927.

2. B. Das, B.K. Mishra, S. Angadi, S.K. Pradhan, S. Prakash, and J. Mohanty: *Waste Manag. Res. J. Int. Solid Wastes Public Clean. Assoc. Iswa*, 2010, vol. 28, pp. 56167.
3. M.E. Schlesinger, M.J. King, K.C. Sole, and W.G. Davenport, *Extractive Metallurgy of Copper* 5th ed, Elsevier, Oxford, 2011.
4. R. Sridhar, J.M. Toguri, and S. Simeonov: *Metall. Mater. Trans. B*, 1997, vol. 28B, pp. 191200.
5. R. Sharma and R.A. Khan: *J. Clean. Prod.*, 2017, vol. 151, pp. 17992.
6. A. Rusen, A. Geveci, Y.A. Topkaya, and B. Derin: *JOM*, 2016, vol. 68, pp. 232331.
7. M.J. Jones: *Advances in extractive metallurgy and refining*, IMM, London, 1972.
8. P. Spira and N.J. Themelis: *JOM.*, 1969, vol. 21, pp. 3542.
9. J.C. Yannopoulos: *Can. Metall. Q.*, 1971, vol. 10, pp. 291307.
10. J.M. Toguri, N.J. Themelis, and P.H. Jennings: *Can. Metall. Q.*, 1964, vol. 3, pp. 19720.
11. M.E. Schlesinger, M.J. King, A.W. Davenport, and K.C. Sole, *Extractive Metallurgy of Copper*, 5th ed. Elsevier, New York, 2011.
12. H. Jalkanen, J. Vehviläinen, and J. Poijärvi: *Scand. J. Metall.*, 2003, vol. 32, pp. 6570.
13. N. Cardona, P. Coursol, P.J. Mackey, and R. Parra: *Can. Metall. Q.*, 2011, vol. 50, pp. 31829.
14. M. Kucharski: *Arch. Hut.*, 1987, vol. 32, pp. 30723.
15. H.P. Rajcevic and W.R. Opie: *JOM*, 1982, vol. 34, pp. 5456.
16. A. Moreno, G. Sánchez, A. Warczok, and G. Riveros, Proc. Conf. Copper 2003, London, Metallurgical Society of CIM, 2003, vol. IV, pp. 475–92.
17. A. Warczok, G. Riveros, P. Echeverría, C.M. Díaz, H. Schwarze, and G. Sánchez: *Can. Metall. Q.*, 2013, vol. 41, pp. 46573.
18. V. Montenegro, T. Fujisawa, A. Warczok, and G. Riveros, *Metallurgical and Materials Processing: Principles and Technologies*, 2003, High-Temperature Metal Production, vol 2, pp. 199–09.
19. A. Warczok, G. Riveros, and V. Montenegro, Proc. 5th Int. Conf. Copper 2003, Santiago, Chile, November 30–December 3, 2003, pp. 1–17.

20. A. Warczok and T.A. Utigard: *Metall. Mater. Trans. B.*, 1995, vol. 26, pp. 116573.
21. M.S. Bafghi: *ISIJ Int.*, 2007, vol. 32, pp. 108490.
22. A. Mitrašinović: *JOM*, 2017, vol. 69, pp. 16.
23. A. Warczok and T.A. Utigard: *Can. Metall. Q.*, 2013, vol. 37, pp. 2739.
24. J.H. Heo, Y. Chung, and J.H. Park: *J. Clean. Prod.*, 2016, vol. 137, pp. 77787.
25. A.A. Lykasov, G.M. Ryss, D.G. Sharafutdinov, and A.Y. Pogodin: *Izvest. Vyss. Uchebnykh Zaved. Chernaya Metall.*, 2016, vol. 59, pp. 597 607 .
26. D. Busolic, F. Parada, R. Parra, M. Sanchez, J. Palacios, and M. Hino: *Miner. Process. ExtrMetall.*, 2011, vol. 120, pp. 3236.
27. H.F. Yang, L.L. Jing, and C.G. Dang: *Chin. J. Nonferrous Met.*, 2011, vol. 21, pp. 116570.
28. R.W. Ruddle: *The Physical Chemistry of Copper Smelting*, IMM, London, 1953.
29. C.P. Liu: *Nonferrous Metals: Extr. Metall.*, 1975, vol. 8, pp. 3645 (In Chinese).
30. L. Bodnar, S. Cempa, K. Tomasek, and L. Bobok, *Chem. Pap.* 1978, vol. 32(6), pp. 798–809.
31. J.O. Bockris and D.C. Lowe: *Proc. R. Soc. A.*, 1954, vol. 226, pp. 42335.
32. G.H. Kaiura, J.M. Toguri, and G. Marchant: *Can. Metall. Q.*, 2013, vol. 16, pp. 15660.
33. P. Taskinen, K. Seppälä, J. Laulumaa, and J. Poijärvi, *Min. Proc. Ext. Met.*, 1997, vol. 110, pp. 94–100.
34. J. Matousek: *JOM*, 2012, vol. 64, pp. 131420.
35. S.W. Ip and J.M. Toguri: *Metall. Trans. B.*, 1992, vol. 23, pp. 30311.
36. P.K. Iwamasa and R.J. Fruehan: *ISIJ Int.*, 1996, vol. 36, pp. 131927.
37. N. Cardona, P. Coursol, J. Vargas, and R. Parra: *Can. Metall. Q.*, 2013, vol. 50, pp. 33040.
38. S.A. Degterov and A.D. Pelton: *Metall. Mater. Trans. B.*, 1999, vol. 30B, pp. 103344.
39. D.C. Lynch, S. Akagi, and W.G. Davenport: *Metall. Trans. B.*, 1991, vol. 22, pp. 67788.